Mechanical stability of TiO_2 polymorphs under pressure: *ab initio* calculations

2008 J. Phys.: Condens. Matter 20 345218

(http://iopscience.iop.org/0953-8984/20/34/345218)

J. Phys.: Condens. Matter **20** (2008) 345218 (7pp) doi:10.1088/0953-8984/20/34/345218

Mechanical stability of TiO_2 polymorphs under pressure: *ab initio* calculations

L Koči[1], D Y Kim[1], J S de Almeida[1], M Mattesini[2], E Isaev[1,3] and R Ahuja[1,4]

[1] Condensed Matter Theory Group, Physics Department, Uppsala University, Box 530, SE-751 21 Uppsala, Sweden
[2] Departamento de Física de la Tierra, Astronomía y Astrofísica I, Universidad Complutense de Madrid, E-28040 Madrid, Spain
[3] Theoretical Physics Department, Moscow State Institute of Steel and Alloys, 4 Leninskii prospect, Moscow 119049, Russia
[4] Applied Materials Physics, Department of Materials Science and Engineering, The Royal Institute of Technology, SE-100 44 Stockholm, Sweden

Received 14 March 2008, in final form 23 June 2008
Published 6 August 2008
Online at stacks.iop.org/JPhysCM/20/345218

Abstract
First-principles calculations using plane-wave basis sets and ultrasoft pseudopotentials have been performed to study the mechanical stabilities of the rutile, pyrite, fluorite and cotunnite phases of titanium dioxide (TiO_2). For these polymorphs, we have calculated the equilibrium volumes, equations of state, bulk moduli and selected elastic constants. Compared to the three phases rutile, pyrite and fluorite, the recently discovered cotunnite phase shows the highest c_{44} for all pressures considered. Cotunnite also shows the highest bulk modulus amongst the four studied phases at an ambient pressure of $B_0 = 272$ GPa.

1. Introduction

Titanium dioxide (TiO_2) exists in a large number of polymorphs, including the abundant rutile, anatase and brookite phases [1] and the high-pressure columbite [2], baddeleyite [3] and cotunnite [4] (c-TiO_2) structures. The recently discovered cotunnite-structured titanium dioxide is the hardest oxide known [4] and may have a hardness approaching that of diamond [2, 5]. Therefore, c-TiO_2 could be a possible substitute for cubic zirconia, ZrO_2 (also known as artificial diamond). Furthermore, due to its rigidity and compressibility reluctance, c-TiO_2 could attract the interests of the drilling industry, where transition-metal carbides and nitrides are frequently used for cutting tools and wear-resistant coatings [6]. Thus, continued research on the properties of c-TiO_2 is highly interesting.

The possibility to quench high-pressure types of TiO_2 to ambient conditions is of great importance for practical applications [7]. As an example, dye-sensitized solar cells (DSSC) benefit from a light-to-electricity efficiency, environmental friendliness and cheap production [8–10]. The anatase phase of TiO_2 has shown to improve the photoelectrochemical properties of the cells, replacing glass as a substrate material. The advantage of using the dioxide in photoelectrodes is its resistance to corrosion and sinterability at high temperatures. However, as an optimal bandgap E_g for electrodes is approximately 2 eV [11], TiO_2 shows limited absorption due to its bandgap of 3.0–3.2 eV [12, 13]. Although studies of TiO_2 doped with In_2O_3 have shown that E_g could be lowered from 2.9 to 2.5 eV [14], doped systems suffer from a lower photoactivity.

These deficiencies make the findings from Mattesini *et al* [15] of a cubic form of TiO_2 at $P = 48$ GPa, $T = 1900$–2100 K interesting, as optical property calculations of the cubic phases fluorite and pyrite have indicated important optical absorptive transitions in the visible light region [7]. The authors have shown that the two cubic TiO_2 phases present absorptions that are considerably more intense than rutile in the wavelength range between 380 and 450 nm. As fluorite and pyrite could be stabilized over the high-pressure c-TiO_2 [15], continued research of these polymorphs is highly motivated.

Another application for TiO_2 is the considered replacement of SiO_2 in dynamic random access memory (DRAM) storage capacitors, as the advantage of TiO_2 lies in its high dielectric constants. Furthermore, the comparison of the rutile phase of TiO_2 with minerals found in the Earth's mantle such as, for example, stishovite (SiO_2) is of interest in geophysics [1].

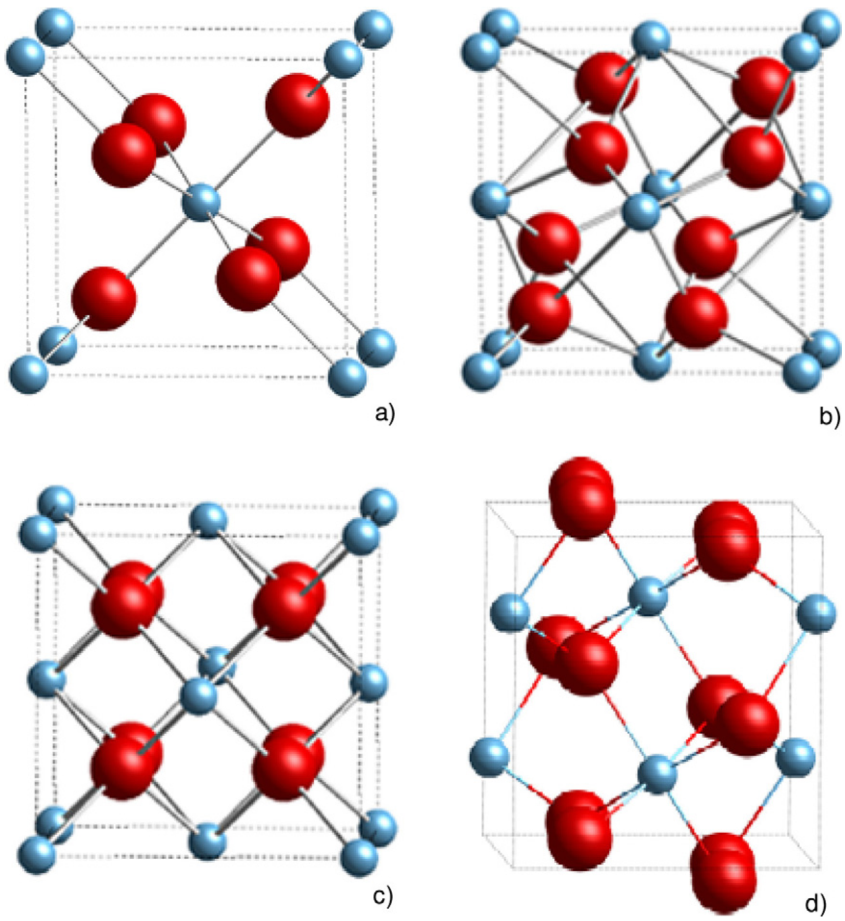

Figure 1. The phases of TiO_2 studied here: (a) rutile, (b) pyrite, (c) fluorite and (d) cotunnite. The large, red spheres represent the O atoms, and the small, blue spheres the Ti atoms.
(This figure is in colour only in the electronic version)

Several experimental studies have been conducted to explore the rich phase diagram of TiO_2. The transformation from the anatase to the columbite phase has been detected at 2.6–8 GPa from Raman spectroscopy [16, 17] and x-ray diffraction [2]. With the rutile form as the initial structure, the transformation was found around 10 GPa [18, 19]. By diamond-anvil cell (DAC) experiments on polycrystalline anatase, the transform to the baddeleyite structure was found at about 13 GPa [20], whereas columbite transforms into baddeleyite at approximately the same pressure (12–17 GPa) [16, 19]. The free energy calculations of Sasaki [21] have indicated the rutile–columbite–baddeleyite transition pressures to be 7.5 and 26 GPa, respectively, whereas Muscat *et al* [1] have shown the columbite–baddeleyite–cotunnite pressures to be 21, 31 and 63 GPa, respectively. Up to 70 GPa, the pyrite and fluorite showed to be less stable than the other polymorphs studied. These results at 0 K in combination with the experimental results at high temperatures, which indeed reveal a cubic phase in this pressure range, imply uncertainties. Therefore, together with the promising properties of the high-pressure forms of TiO_2, we have performed calculations on the rutile, fluorite, pyrite and cotunnite phases.

The results are followed by a discussion and a conclusion. In the next two sections, the methods are described, including the EOS, the elastic constant calculations and the code used. The results are followed by the conclusions.

2. Equation of state and elastic constants

To calculate the EOS as presented in figure 2, the third-order Birch–Murnaghan EOS was used [22, 23]:

$$E = E_0 + \tfrac{3}{2}B_0V_0\left[\tfrac{3}{2}(\chi-1)x^{\frac{2}{3}} + \tfrac{3}{4}(1-2\chi)x^{\frac{4}{3}} + \frac{1}{2}\chi x^{\frac{6}{3}} - \frac{2\chi-3}{4}\right], \quad (1)$$

$$P = \tfrac{3}{2}B_0[x^{\frac{7}{3}} - x^{\frac{5}{3}}][1 + \chi(x^{\frac{2}{3}} - 1)], \quad (2)$$

and

$$B = \tfrac{3}{2}B_0[\tfrac{7}{3}x^{\frac{7}{3}} - \tfrac{5}{3}x^{\frac{5}{3}}][1 + \chi(x^{\frac{2}{3}} - 1)] + \tfrac{3}{2}B_0[x^{\frac{7}{3}} - x^{\frac{5}{3}}][1 + \tfrac{2}{3}\chi x^{\frac{2}{3}}], \quad (3)$$

where $x = V_0/V$ and $\chi = \frac{3}{4}(B_0' - 4)$. The reason for choosing the Birch–Murnaghan EOS is due to the extensive use of the method in experiments to get bulk moduli from pressure–volume data.

To deduce the elastic moduli, strains were applied to the lattices, yielding energy deviations from equilibrium. If a

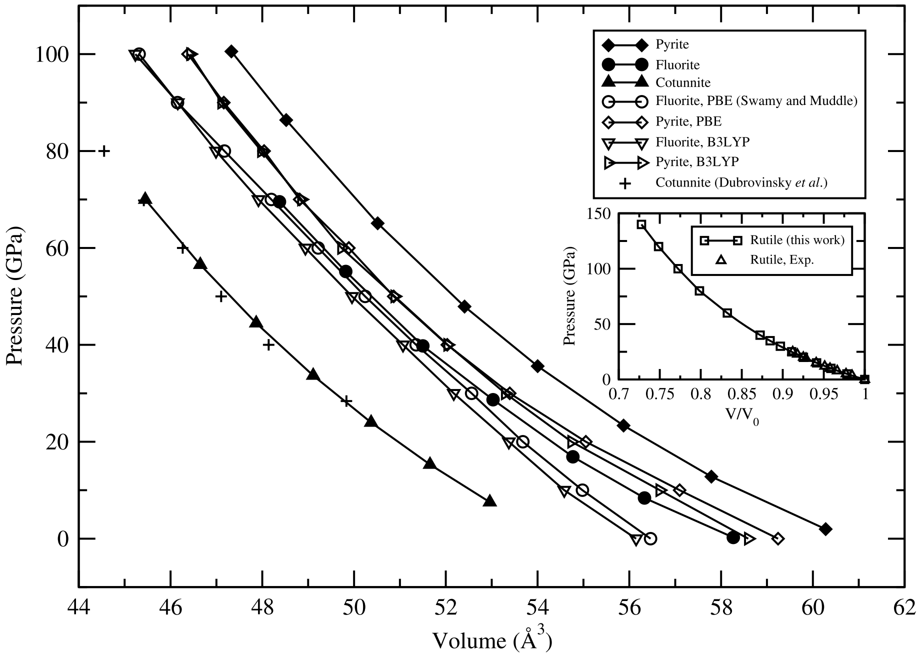

Figure 2. Equation of state (EOS) with pressure as a function of volume for the pyrite, fluorite and cotunnite phases. In the inset, the pressure as a function of relative volume is compared to the best fit from the combined experimental rutile results [51, 53, 54]. The volume is expressed in two TiO_2 formula units.

Table 1. Strains for the rutile, fluorite, pyrite and cotunnite phases of TiO_2.

Phase	Parameters	$[E(V,e)-E(V_0,0)]/V_0$
Rutile	$e_2=e_1$	$(c_{11}+c_{12})e_1^2$
	$e_2=e_1,\ e_3=\frac{1}{(1+e_1)^2}-1$	$(c_{11}+c_{12}+2c_{33}-4c_{13})e_1^2$
	e_3	$\frac{1}{2}c_{33}e_3^2$
	$e_1=\sqrt{\frac{1+x}{1-x}}-1,\ e_2=\frac{-e_1}{1+e_1}$	$(c_{11}-c_{12})x^2$
	$e_5=e_4,\ e_3=e_4^2/4$	$c_{44}e_4^2$
	$e_6,\ e_1=e_2=\sqrt{1+e_6^2/4}-1$	$\frac{1}{2}c_{66}e_6^2$
Fluorite	$2e_6,\ e_3=\frac{1}{1-e_6^2}-1$	$2c_{44}e_6^2$
Pyrite	$2e_6,\ e_3=\frac{1}{1-e_6^2}-1$	$2c_{44}e_6^2$
Cotunnite	$e_2=e_3=\frac{1}{2}\sqrt{4+e^2}-1,\ e_4=-e$	$\frac{1}{2}c_{44}e_4^2$

Taylor expansion is performed for the energy $E(V,e)$, where V is the volume and e a small strain of the lattice, the truncated energy becomes

$$E(V,e)=E(V_0,0)+V_0\left(\sum_i \tau_i e_i \eta_i+\frac{1}{2}\sum_{ij} c_{ij} e_i \eta_i e_j \eta_j\right), \tag{4}$$

where V_0 is the equilibrium volume and τ_i are elements in the stress tensor. Following the Voigt notation, $\eta_i=1$ if $i=1,2$ or 3 and $\eta_i=2$ if $i=4,5$ or 6. The distortions were applied according to the rule [24]

$$\mathbf{a}'=[\mathbf{I}+\boldsymbol{\epsilon}(e)]\mathbf{a}, \tag{5}$$

where $\mathbf{I}$ is the 3×3 identity matrix, $\mathbf{a}$ ($\mathbf{a}'$) are the undistorted (distorted) lattice vectors and $\boldsymbol{\epsilon}(e)$ is the strain component matrix described as

$$\boldsymbol{\epsilon}(e)=\begin{pmatrix} e_1 & \frac{1}{2}e_6 & \frac{1}{2}e_5 \\ \frac{1}{2}e_6 & e_2 & \frac{1}{2}e_4 \\ \frac{1}{2}e_5 & \frac{1}{2}e_4 & e_3 \end{pmatrix}. \tag{6}$$

The distortions for the four studied structures rutile, fluorite, pyrite and cotunnite are shown in table 1. Neglecting the first-order term in the distortion e, equation (4) can be written as

$$\frac{E(V,e)-E(V_0,0)}{V_0}=\frac{1}{2}\sum_{ij} c_{ij} e_i \eta_i e_j \eta_j. \tag{7}$$

To calculate the elastic constants from equation (7), the $[E(V,e)-E(V_0,0)]/V_0$ expressions were fitted to a second-order function of the distortion e by means of least squares polynomial approximations. It is worth noting that the first and third strain in table 1, although not being volume conserving, have tetragonal symmetry together with the volume conserving second strain. The c_{ij}:s calculated from these strains are the only elastic constants needed to calculate the bulk modulus B. The last three strains do not conserve the symmetry, but are volume conserving. This is quite important when one deals with elastic constant calculations under pressure as we studied the pressure dependence of c_{44} for the cotunnite phase.

Table 2. Structural parameters of rutile, fluorite, pyrite and cotunnite TiO_2 at 0 GPa (unless specified). Lengths are in Å and volumes in Å^3 for two TiO_2 formula units. For rutile, $a = b$ and for fluorite and pyrite, $a = b = c$.

Rutile	*a*	*b*	*c*	Volume
PBE (this work)	4.681		3.005	65.855
PW91 [1, 40, 48]	4.624–4.690		2.981–2.992	63.821–65.768
Exp. [34, 37]	4.587–4.594		2.954–2.959	62.154–62.435
Fluorite				
PBE (this work)	4.882			58.220
PBE [47]	4.833			56.375
PW91 [1]	4.897			58.706
B3LYP [47]	4.824			56.065
Exp. [15]	4.870			57.750
Pyrite				
PBE (this work)	4.942			60.340
PBE [47]	4.911			59.310
PW91 [1]	4.894			58.592
B3LYP [47]	4.893			58.630
Cotunnite				
PBE (this work, 0 GPa)	5.456	3.158	6.303	54.303
PBE (this work, 60 GPa)	5.187	3.003	5.994	46.683
Exp. [4] (61 GPa)	5.163	2.989	5.966	46.266

3. Method

Total energy calculations were performed in the framework of the density functional theory [25] (DFT) as it is implemented in the QuantumESPRESSO code [26] in conjunction with the plane-wave (PW) basis set and ultrasoft pseudopotentials. PWs with cutoff energies up to 60 Ryd were included in the basis set, and additional PWs with kinetic energy up to 450 Ryd were used in order to describe the augmented charge. An ultrasoft pseudopotential [27] for Ti was generated using single excited atomic configurations with semicore $3s^2 3p^6$ states and cutoff radii $r_s = r_p = r_d = 1.8$. The oxygen pseudopotential was generated [28] by means of the Rabe–Rappe–Kaxiras–Joannopoulos method [29] on the base of Bessel functions. The gradient-corrected exchange–correlation functional was used in the form of Perdew–Becke–Ernzerhof (PBE) [30]. Lattice parameters and atomic positions of TiO_2 phases under high pressure were optimized by means of the variable cell shape method [31, 32]. By means of several tests of convergence, the integration over the Brillouin zone was carried out using a $12 \times 12 \times 12$ k-point grid for the fluorite and the pyrite phases, and a $4 \times 4 \times 4$ grid for the rutile and the cotunnite structures. In the simulations, the tetrahedral method with Blöchl corrections [33] was used. As a convergence threshold for total energy calculations, we chose 10^{-10} Ryd.

4. Results

By relaxing the rutile structure at ambient pressure, the parameters were found to be $a = 4.68$ Å, $c = 3.01$ Å and $u = 0.304$. For fluorite and pyrite, the parameters were found to be 4.88 and 4.94 Å, respectively. For cotunnite, $a = 5.46$, $b = 3.16$ and $c = 6.30$ Å. The calculated structural parameters of the rutile, fluorite, pyrite and cotunnite phases are shown in table 2. In this work, the calculations for rutile overestimate the lattice parameter a by 2.0% and c by 1.7% compared to experimental data [34]. This is consistent with the findings of Muscat *et al* [1] who have reported the trend of GGA overestimating both a and c. Furthermore, this deviation from the equilibrium volume with the exchange–correlation functional has been observed for two other dioxides, namely SiO_2 [35] and ZrO_2 [36]. It is also worth noting that the c/a ratio from the calculations in this work, 0.642, is in perfect agreement with the experimentally found ratio 0.644 from both Burdett *et al* [34] and Isaak *et al* [37].

For the fluorite and pyrite phases, the theoretical data available in the literature varies as several exchange–correlation methods (LDA, GGA, HF) have been used [1, 38, 39]. For fluorite, the parameters and volumes calculated in this work agree almost perfectly with the cited GGA data [1], whereas a slight overestimation is seen compared to LDA data [1, 38, 40] and Hartree–Fock theory [1]. For pyrite, the same trend is shown as for the fluorite calculations. The compression of the cotunnite structure at ambient conditions to 60 GPa indicates an almost perfect match, as the deviation from experiment is less than 1% [4]. The EOS with pressure as a function of volume for the pyrite, fluorite and cotunnite phases is shown in figure 2. Shown in the inset, the theoretical and the experimental EOS for the rutile are practically overlapping, in spite of somewhat larger lattice parameters calculated.

The elastic constants calculations for the rutile phase are in reasonable agreement with experiments [37, 39, 41] and the resonant sphere technique (RST) [42], as shown in table 3. All studied elastic constants are positive and the mechanical stability restrictions including the inequalities $c_{11} > c_{12}$ and $c_{11} + c_{33} - 2c_{13} > 0$ are fulfilled. As the experimental samples are polycrystalline rather than monocrystalline, it is worth estimating the upper and lower bounds for the bulk modulus of

Table 3. Elastic constants and bulk and shear moduli bounds of rutile at 0 GPa.

Rutile	c_{44}	c_{11}	c_{33}	c_{12}	c_{13}	c_{66}	B_R	B_V	G_R	G_V
PBE (this work)	113	276	483	154	152	211	205	217	107	126
RST [42]	123	267	483	176	148	193	208	218	98	124
Exp. [37, 39, 41]	123–124	267–271	479–484	175–181	147–150	189–195	208–211	218–220	95–99	123–125

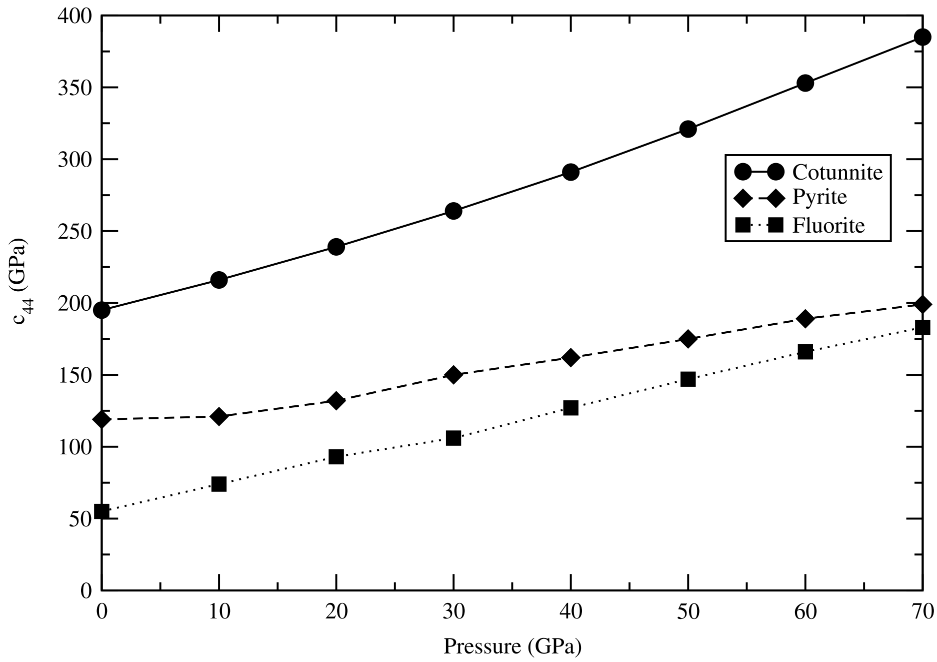

Figure 3. Elastic constant c_{44} as a function of pressure for the pyrite, fluorite and cotunnite phases.

the tetragonal rutile phase. The bounds are defined according to the Voigt [43] and Reuss [44] approximations, respectively:

$$B_V = \tfrac{1}{9}[2(c_{11}+c_{12})+c_{33}+4c_{13}], \quad (8)$$

and

$$B_R = \frac{(c_{11}+c_{12})c_{33}-2c_{13}^2}{c_{11}+c_{12}+2c_{33}-4c_{13}}. \quad (9)$$

Inserting the elastic constants from table 3 in equations (8)–(9) gives $B_V = 217$ GPa and $B_R = 205$ GPa, which are in good agreement with both theory [42] and experiment [37, 39, 41]. It is instructive also to estimate the upper shear modulus according to Voigt:

$$G_V = \tfrac{1}{15}(2c_{11}+c_{33}-c_{12}-2c_{13}+6c_{44}+3c_{66}), \quad (10)$$

and the lower shear modulus after Reuss:

$$G_R = 15/(8s_{11}+4s_{33}-4s_{12}-8s_{13}+6s_{44}+3s_{66}), \quad (11)$$

where s_{ij} are the constants

$$\begin{aligned} s_{11}+s_{12} &= c_{33}/C, & s_{11}-s_{12} &= 1/(c_{11}-c_{12}), \\ s_{13} &= -c_{13}/C, & s_{33} &= (c_{11}+c_{12})/C, \\ s_{44} &= 1/c_{44}, & s_{66} &= 1/c_{66}, \end{aligned} \quad (12)$$

and

$$C = c_{33}(c_{11}+c_{12})-2c_{13}^2. \quad (13)$$

Furthermore, the Hill (G_H) shear modulus is an averaged value of G_V and G_R [24]. We found $G_V = 126$ GPa, $G_R = 107$ GPa and $G_H = 117$ GPa. Although G_V matches the cited data in table 3, the G_R from the calculations in this work is somewhat overestimated due to a relatively high $c_{11} - c_{12}$ difference. From equation (12), this yields a small s_{11} term and a small negative s_{12} term. As these terms are in the denominator of equation (9), the modulus increases.

The c_{44} calculations as a function of pressure up to 70 GPa for the pyrite, fluorite and cotunnite phases are shown in figure 3. As expected, the cotunnite structure indicates greater rigidity compared to the cubic types.

The calculated bulk modulus B_0 and its derivative B' from equation (3) for the rutile phase shown in table 4 is in good agreement with both theory and experiment. Furthermore, in combination with the results in table 3, one can easily check that the inequality $\frac{1}{3}(c_{12}+2c_{13}) < B_0 < \frac{1}{3}(2c_{11}+c_{33})$ for the bulk modulus is also fulfilled. For the cubic forms pyrite and fluorite, the calculated B_0 data are somewhat low compared to LCAO-HF calculations [1, 45, 46]. Although the bulk modulus for the fluorite phase is overestimated compared to experiment [15], it is well below the remarkably high $B_0 = 395$ GPa as reported recently by Swamy and Muddle [47]. For cotunnite, equation (3) yields $B_0 = 272$ GPa with $B' = 4.09$. The experimentally found $B_0 = 431$ GPa with the extremely low $B' = 1.35 \pm 0.1$ [4] could be a result of suffering from a limited measurement precision.

Table 4. Bulk properties (in GPa) of the rutile, pyrite, fluorite and cotunnite phases of TiO_2 at 0 GPa.

Method		Rutile	Pyrite	Fluorite	Cotunnite
PBE (this work)	B_0	200	239	246	272
	B'	5.75	4.19	4.41	4.09
PBE [47]	B_0	215 ± 1	220 ± 4	395 ± 4	
	B'	5.35 ± 0.16	4.86 ± 0.11	1.75 ± 0.05	
B3LYP [47]	B_0	224 ± 8	258 ± 2	390 ± 4	
	B'	5.64 ± 0.90	4.35 ± 0.04	2.06 ± 0.06	
LCAO-HF [1, 45, 46]	B_0	239–304	318 ± 10	331 ± 10	380 ± 10
LCAO-LDA [1, 45, 49]	B_0	209–264			
PW-LDA [38, 40, 50]	B_0	240–244		282–287	
Exp. [4, 15, 37, 51, 52]	B_0	211–230		202 ± 5	431 ± 10
	B'	6.76		1.3 ± 0.1	1.35 ± 0.1

Dubrovinsky *et al* [4] predict cotunnite to be the most stable phase at pressures above 70 GPa, having a lower Gibbs free energy than the OI (space group $Pbca$) and MI ($P2_1/c$) phases. Furthermore, the authors have reported the possibility of preserving the cotunnite type at ambient pressure by cryogenic quenching. Muscat *et al* [1] show lower energy for cotunnite than for baddeleyite at 65 GPa.

As TiO_2 reveals a rich phase diagram as a function of pressure, there are many uncertainties about the polymorphs. The fluorite and pyrite types [15] were synthesized in high-temperature regimes (∼2000 K) where kinetic effects may be dominant. The cotunnite phase, however, obtained by Dubrovinsky *et al* [4] was found at much lower temperatures (∼1000 K). Therefore, thermal EOS calculations could change the enthalpy-based stability regimes of the forms studied.

5. Conclusions

In this work, we have investigated the structural parameters, elastic constants and bulk moduli for the rutile, pyrite, fluorite and cotunnite phases of TiO_2. The bulk moduli and elastic constant calculations for the rutile phase are in good agreement with previous studies. For the high-pressure types fluorite, pyrite and cotunnite, the structural parameters are in agreement with the presented data. The c_{44} elastic constant is highest for cotunnite, followed by pyrite and fluorite. Comparing the calculated bulk moduli for the studied structures, the rutile phase is softer than pyrite and fluorite, and the cotunnite phase could indeed be very hard.

Acknowledgments

This work was supported by the Swedish Research Council (VR), STINT and Kungliga Vetenskapsakademien (KVA). One of the authors (MM) wishes to acknowledge the Spanish Ministry of Science and Technology (MCyT) for financial support through the Ramón y Cajal program. JSA acknowledges support from the Brazilian National Research Council (CNPq). EII thanks the Russian Foundation for Basic Researches (RFBR, grants 05-02-17464, 07-02-01266 and 06-02-17542), and the Netherlands Organization for Scientific Researches (NWO, grant 047.016.005) for financial support.

References

[1] Muscat J, Swamy V and Harrison N M 2002 *Phys. Rev.* B **65** 224112
[2] Haines J and Leger J M 1993 *Physica* B **192** 233
[3] Sato H, Endo S, Sugiyama M, Kikegawa T, Shimomura O and Kusuba K 1991 *Science* **251** 786
[4] Dubrovinsky L S, Dubrovinskaia N A, Swamy V, Muscat J, Harrison N M, Ahuja R, Holm B and Johansson B 2001 *Nature* **410** 653
[5] Olsen J S, Gerward L and Liang J Z 1999 *J. Phys. Chem. Solids* **60** 229
[6] Jhi S-H, Ihm J, Louie S G and Cohen M L 1999 *Nature* **399** 132
[7] Mattesini M, de Almeida J S, Dubrovinsky L, Dubrovinskaia N, Johansson B and Ahuja R 2004 *Phys. Rev.* B **70** 115101
[8] Mor G K, Shankar K, Paulose M, Varghese O K and Grimes C A 2006 *Nano Lett.* **6** 215
[9] Kanga M G, Parka N-G, Ryua K S, Changa S H and Kim K-J 2006 *Sol. Energy Mater. Sol. Cells* **90** 574
[10] Bach U, Lupo D, Comte P, Moser J E, Weissörtel F, Salbeck J, Spreitzer H and Grätzel M 1998 *Nature* **395** 583
[11] Bak T, Nowotny J, Rekas M and Sorrell C C 2002 *Int. J. Hydrog. Energy* **27** 991
[12] Fujishima A and Honda K 1972 *Nature* **2** 37
[13] Nozik A J 1975 *Nature* **257** 383
[14] Babu K S C, Sing D and Srivastava O N 1990 *Semicond. Sci. Technol.* **5** 364
[15] Mattesini M, de Almeida J S, Dubrovinsky L, Dubrovinskaia N, Johansson B and Ahuja R 2004 *Phys. Rev.* B **70** 212101
[16] Lagarec K and Desgreniers S 1995 *Solid State Commun.* **94** 519
[17] Ohsaka T, Yamaoka S and Shimomura O 1979 *Solid State Commun.* **30** 345
[18] Mammone F, Sharma S K and Nicol M 1980 *Solid State Commun.* **34** 799
[19] Arashi H 1992 *J. Phys. Chem. Solids* **53** 355
[20] Arlt T, Bermejo M, Blanco M A, Gerward L, Jiang J Z, Olsen J S and Recio J M 2000 *Phys. Rev.* B **61** 14414
[21] Sasaki T 2002 *J. Phys.: Condens. Matter* **14** 10557
[22] Birch F 1947 *Phys. Rev.* B **71** 809
[23] Birch F 1978 *J. Geophys. Res.* **83** 1257
[24] Mehl M J, Osburn J E, Papaconstantopoulos D A and Klein B M 1990 *Phys. Rev.* B **41** 10311
[25] Hohenberg P and Kohn W 1964 *Phys. Rev.* **136** 864
[26] Baroni S *et al* 1997 http://www.pwscf.org
[27] Vanderbilt D 1990 *Phys. Rev.* B **41** 7892
[28] 1997 For more details see http://www.pwscf.org/pseudo.htm
[29] Rappe A M, Rabe K M, Kaxiras E and Joannopoulos J D 1990 *Phys. Rev.* B **41** 1227
[30] Perdew J P, Burke K and Ernzerhof M 1996 *Phys. Rev. Lett.* **77** 3865

[31] Wentzcovitch M 1991 *Phys. Rev.* B **44** 2358
[32] Bernasconi M, Chiarotti G L, Focher P, Scandolo S, Tosatti E and Parrinello M 1995 *J. Phys. Chem. Solids* **56** 501
[33] Blöchl P E, Jepsen O and Andersen O K 1994 *Phys. Rev.* B **49** 16223
[34] Burdett J K, Hughbanks T, Miller G J, Richardson J W and Smith J W 1987 *J. Am. Chem. Soc.* **109** 3639
[35] Demuth T, Jeanvoine Y, Hafner J and Ángyán J G 1999 *J. Phys.: Condens. Matter* **11** 3833
[36] Christensen A and Carter E A 2001 *J. Chem. Phys.* **114** 5816
[37] Isaak D G, Carnes J D, Anderson O L, Cynn H and Hake E 1998 *Phys. Chem. Miner.* **26** 31
[38] Dewhurst J K and Lowther J E 1996 *Phys. Rev.* B **54** R3673
[39] Grimsditch M H and Ramdas A K 1976 *Phys. Rev.* B **14** 1670
[40] Milman V 1997 *Properties of Complex Inorganic Solids* (New York: Plenum)
[41] Manghnani M H 1969 *J. Geophys. Res.* **74** 4317
[42] Suzuki I, Oda H, Isoda S, Saito T and Seya K 1992 *J. Phys. Earth.* **40** 601
[43] Voight W 1928 *Lehrbuch der Kristallphysik* (Leipzig: Teubner)
[44] Reuss A 1929 *Z. Angew. Math. Mech.* **9** 49
[45] Reinhard P, Hess B A and Causà M 1996 *Int. J. Quantum Chem.* **58** 297
[46] Rosciszewski K, Doll K, Paulus B, Fulde P and Stoll H 1998 *Phys. Rev.* B **57** 14667
[47] Swamy V and Muddle B C 2007 *Phys. Rev. Lett.* **98** 035502
[48] Lindan P J D, Harrison N M, Gillan M J and White J A 1997 *Phys. Rev.* B **55** 15919
[49] Mo S D and Ching W Y 1995 *Phys. Rev.* B **51** 13023
[50] Glassford K M and Chelikowsky J R 1992 *Phys. Rev.* B **46** 1284
[51] Ming L C and Manghnani M H 1979 *J. Geophys. Res.* **84** 4777
[52] Gerward L and Olsen J S 1997 *J. Appl. Crystallogr.* **30** 259
[53] McQueen R G, Jamieson J C and Marsh S P 1967 *Science* **155** 401
[54] Sato Y 1997 *High-Pressure Research: Applications in Geophysics* ed M H Manghnani and S Akimoto (New York: Academic) p 307